Thermal Conductivity of Polymer-Based Composites with Magnetic Aligned Hexagonal Boron Nitride Platelets

Chao Yuan, Bin Duan, Lan Li, Bin Xie, Mengyu Huang, and Xiaobing Luo*

School of Energy and Power Engineering, Huazhong University of Science and Technology, Wuhan 430074, China

S Supporting Information

ABSTRACT: Hexagonal boron nitride (hBN) platelets are widely used as the reinforcing fillers for enhancing the thermal conductivity of polymer-based composites. Since hBN platelets have high aspect ratio and show a highly anisotropic thermal property, the thermal conductivity of the hBNs-filled composites should be strongly associated with the platelets' orientation. However, the orientation effect has been explored less frequently due to the technical difficulties in precontrol of the platelets' orientation in the polymer matrix. In this paper, we report the use of magnetic fields to assemble the platelets into various microstructures and to study the thermal conductivities of the designed composites. The experimental results showed that thermal conductivities are dramatically different among these composites. For instance, the thermal conductivities of the composites with platelets oriented parallel and perpendicular to the heat flux direction are respectively 44.5% higher and 37.9% lower than that of unaligned composites at the volume fraction of 9.14%. The results were also analyzed by a theoretical model. The model suggests that the orientation of the hBN platelets is the main reason for the variance in the thermal conductivity.

KEYWORDS: *thermal conductivity, polymer-based composites, hexagonal boron nitride, orientation, magnetic alignment*
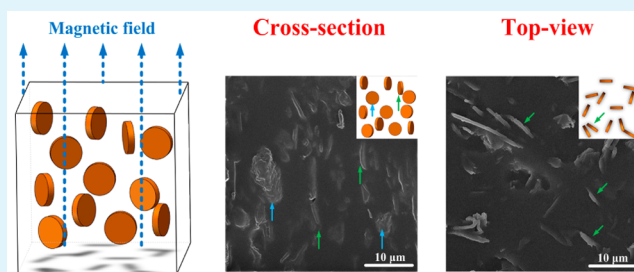
1. INTRODUCTION

Thermally conducting but electrically insulating polymer-based composites have been widely used in electronics for die attachments, encapsulations, and dielectrics.[1−4] These materials are predominantly manufactured by introducing the highly thermally conducting particles, such as ceramics, metals, or metal oxides, into the polymer matrix.[5−9] Nowadays, hexagonal boron nitride (hBN) has been receiving significant attention as the new form of reinforcing filler due to its excellent thermal conductivity and electrically insulating properties. As schematically shown in Figure 1a, hBN is a platelet-shaped particle with a high aspect ratio (D/t) and shows a highly anisotropic thermal property: the in-plane thermal conductivity is about 600 W m^{-1} K^{-1},[10] whereas the through-plane thermal
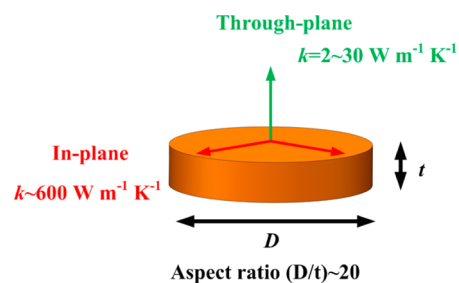
conductivity is only 2−30 W m^{-1} K^{-1}.[10,11] Owing to its significant anisotropies in shape and thermal conductivity, the thermal conductivity of the hBN-filled composites should be strongly associated with the orientation of the hBN. However, the orientation effect has been less studied, and the thermal properties of hBN-filled composites have often been assumed to be isotropic.[12−14]

The orientation effect is less explored due to the technical difficulties in precontrol of the orientation of platelets in the polymer matrix. Several synthetic approaches have been proposed to obtain the well-ordered microstructures in platelet-reinforced composites, including electrical fields,[15] tape-casting,[16] and freeze-casting followed by sintering and polymer infiltration.[17] These approaches usually yield composites that can exhibit highly anisotropic properties but normally require multiple processing steps. The squeezing process is a simple but effective method to control the platelets orientation.[13] The platelets are preferentially aligned parallel to the flow direction of the polymer matrix.[13] However, this method is only for the in-plane alignment and limited to the thin films.

Recently, an attractive strategy was proposed to control filler orientation or position in a matrix.[18] The approach relies on coating the reinforcing particles with superparamagnetic

Figure 1. Representation of the geometry and anisotropic properties of hBN platelets.

nanoparticles to make them magnetically responsive.[18,19] These coated particles exhibit an ultrahigh magnetic response (UHMR)[18] that enables remote control over their orientation under low external magnetic fields in low-viscosity suspending fluids. Such fluids can be then consolidated to fix the magnetically imposed orientation. With this strategy, various microstructures have been achieved in the polymer-based composites.[10,18] Thus, this strategy is suitable for our study.

In this study, the thermal conductivity of hBN-filled composites was investigated as a function of the orientation of the hBN. In the beginning, the composites with through-plane and in-plane aligned hBN platelets were both fabricated with the magnetic alignment method. For the purpose of comparison, the composite with randomly oriented platelets was also prepared without the magnetic control. Then the morphology of those composites was characterized by scanning electron microscopy (SEM), and the degree of orientation was estimated by X-ray diffraction (XRD) measurements. After that, through-plane thermal conductivity (k_T) was measured for those composites. A theoretical model was finally used to fit and analyze the measured results.

2. EXPERIMENTAL SECTION

Preparation of Magnetically Responsive hBN (mhBN) Platelets. hBN platelets are coated with superparamagnetic iron oxide nanoparticles to make them responsive to magnetic fields via a previously reported procedure.[18] hBN platelets, with an averaged diameter (D) of 5 μm, were kindly provided by Momentive. A 4 g portion of hBN platelets was first suspended in 200 mL of deionized water at pH 7. Under continuous stirring, 400 μL of EMG-605 ferrofluid (Ferrotec) diluted with 5 mL of deionized water was added dropwise. The EMG-605 ferrofluid is an aqueous suspension containing iron oxide nanoparticles coated with a cationic surfactant. At pH 7, the hBN platelets have a negative surface charge. Thus, the iron oxide nanoparticles attached to the surface of the platelets through the electrostatic interaction between the positively charged nanoparticles and negatively charged platelets. The suspension was incubated for 1 h to coat the platelets with all the iron oxide nanoparticles. After that, the coated platelets were washed three times with deionized water, by repeatedly changing the supernatant solution after settling of the platelets to the bottom of a glass vial. Subsequently, the magnetized platelets were dried for 12 h at 90 °C in a vacuum.

Preparation of Composites with Controlled Orientation of Reinforcements. Composites with controlled orientation of reinforcements were prepared using the polymer matrix and mhBN platelets. In this report, silicone gel (OE-6550, Dow Corning) was selected as the matrix due to its high thermal and chemical stabilities and low viscosity, which is beneficial for the filler alignment. mhBN platelets was first suspended in silicone gel and stirred for 30 min to be fully dispersed. Then, the curing catalyst was added with stirring. The bubbles introduced during the stirring process were removed by applying alternating cycles of vacuum. After that, the polymer suspension was poured onto a 30 × 30 × 2 mm Teflon mold. To obtain the composites with vertically or horizontally aligned platelets, the mold was placed into a magnetic field of the corresponding direction. The linear, uniform magnetic field was applied using two parallelly arranged custom 200 × 100 mm rectangular solenoids. Figure 2 schematically shows the alignment of mhBN platelets with the magnetic field control. Samples were heated with the magnetic field at 60 °C for 6 h to lower the viscosity of the silicone gel for efficient filler alignment. An annealing step at 150 °C for 6 h was conducted to ensure the full curing of the composites. For comparative purposes, the polymer suspension was also cured without magnetic field to obtain the unaligned composites.

Characterization of mhBN Platelets and mhBN–Silicone Composites. Field-emission scanning electron microscopy (FSEM, Quanta 450 FEG) was used to characterize the morphology of mhBN
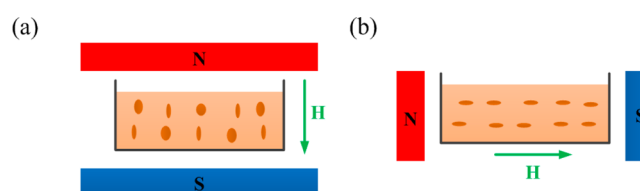

Figure 2. Schematic for (a) through-plane and (b) in-plane alignments of mhBN platelets at the linear and uniform magnetic fields.

platelets at an accelerating voltage of 20 kV. The platelets were first sputtered with a thin layer of graphite before visualization in the instrument. To confirm the presence of iron oxide particles on mhBN platelets, X-ray diffraction (XRD) analysis of the platelets was carried out with X'Pert PRO using Cu Kα radiation (40 kV and 40 mA). To confirm the attachment of iron oxide nanoparticles to the surface of hBN platelet, SEM was carried out using the FEI Nova Nano SEM 450.

The morphology of mhBN–silicone composite surfaces was observed using focused-ion beam scanning electron microscopy (FIB-SEM, Quanta 3D FEG) at an accelerating voltage of 30 kV. Before visualization, a focused-ion beam was used to remove selectively the outer layer of silicone gel to expose the inner mhBN platelets. Then the platelets can be easily visualized from SEM images. XRD analysis of mhBN–silicone composites was also conducted to evaluate the orientation of mhBN platelets in composites. Before the tests, the composites were cut to expose the inner surfaces.

Thermal conductivity is calculated by $k = \alpha C_p \rho$, where α, C_p, and ρ are thermal diffusivity, heat capacity, and density of the sample, respectively. α of the composite was measured with a laser flash method using a LFA 457 (Netzsch) at 25 °C. The geometry of the tested sample is a 10 × 10 × 2 mm cuboid that was cut from the prepared cured composites. Before the test, a thin graphite film is applied on the composite surfaces to increase the energy absorption and the emittance of the surfaces. During the test, heat propagates from the bottom to the top surface of the material. C_p was determined by differential scanning calorimetry (Diamond DSC, PerkinElmer Instruments), and ρ was calculated from the weight and dimensions of the composite.

3. RESULTS AND DISCUSSION

Characterization of mhBN Platelets. Figure 3a shows the FSEM images of mhBN platelets. From this figure, the large aspect ratio (D/t) is found for the platelets. Since the thickness (t) of platelets is estimated to be 250 nm,[10] D/t is approximately equal to 20. The left side of Figure 3b shows a digital photograph of mhBN platelets dispersion in acetone. The right side of Figure 3b presents a facile separation of mhBN platelets from the acetone by an external magnetic field, so this figure illustrates that mhBN platelets respond to the external magnetic field. The presence of iron oxide particles is verified by the XRD pattern of mhBN platelets (Figure 3c), in which the diffraction peaks [(220), (311), (511), (440)] from iron oxide are observed. Figure 3d shows the nanostructure of a mhBN platelet. It reveals that the size of the iron oxide nanoparticles is about 20 nm and further confirms the attachment of nanoparticles to the platelet surface.

Characterization of the Composites with Controlled Orientation of mhBN Platelets. Through-plane-aligned mhBN–silicone (TmhBN–silicone) and in-plane-aligned mhBN–silicone (ImhBN–silicone) were prepared by applying a through-plane and in-plane magnetic field, respectively. For comparative purposes, randomly oriented mhBN–silicone (RmhBN–silicone) was fabricated without the magnetic control. Parts a, b, and c of Figure 4 schematically show the microstructure of the TmhBN–silicone, ImhBN–silicone, and
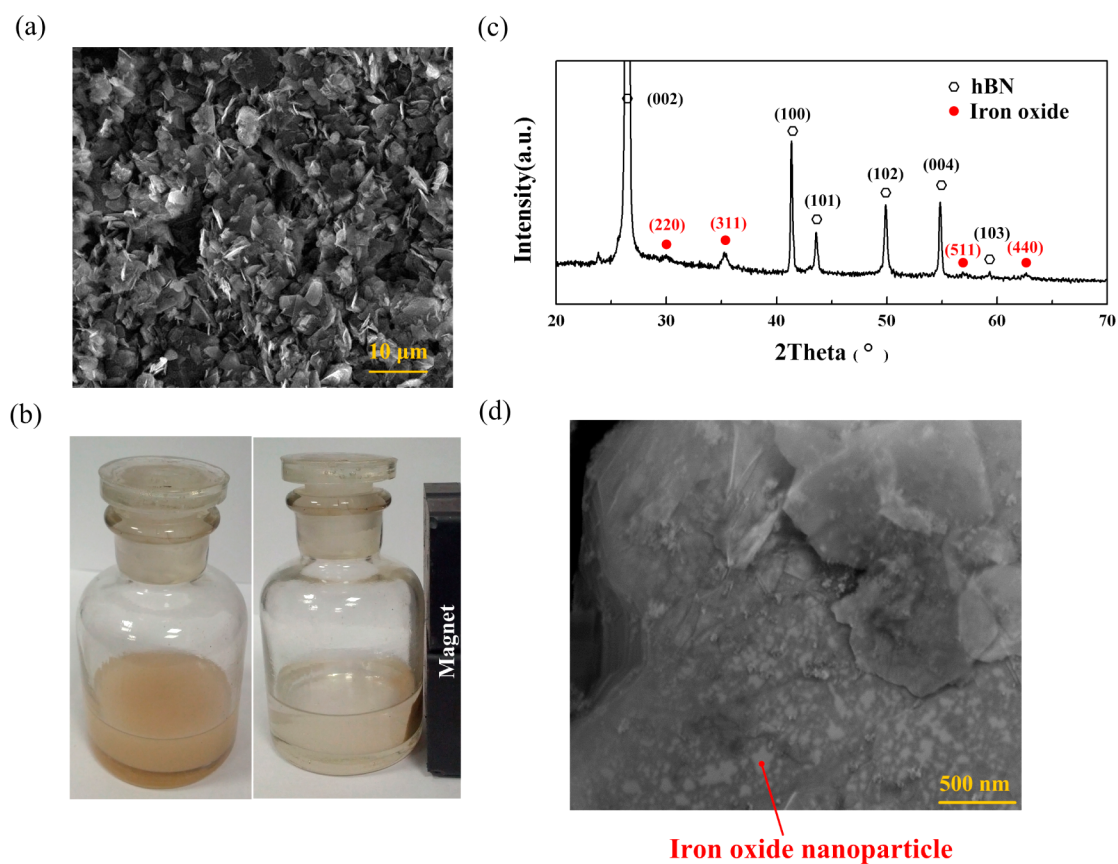
Figure 3. Characterization of mhBN platelets. (a) FSEM image of mhBN platelets. (b) Images of mhBN platelets dispersed in acetone (left) and the separation of platelets from the acetone by an external magnetic field (right). (c) XRD pattern of mhBN platelets; the black hexagons refer to peaks of hBN, and the red circles refer to those of iron oxide nanoparticles. (d) SEM image showing the nanostructure of a mhBN platelet.

RmhBN−silicone composites, respectively, and Table 1 summarizes the representative morphologies of mhBN platelets at cross sectional and top views of those composites. FIB-SEM images of 9.14 vol % mhBN−silicone composites are shown in Figure 4d−i. Parts d and g of Figure 4 give the cross-sectional and top-view FIB-SEM images of TmhBN−silicone, respectively. Figure 4d illustrates that mhBN platelets align along the orientation of the magnetic field. Two representative morphologies of platelets exist in the cross sectional view, 1D vertical rods and 2D plates, which are indicated by green and blue arrows, respectively. In the top view (Figure 4g), most platelets are projected as 1D rods with random orientation. Schematic pictures of the cross-sectional and top view are also given in the insets. It is found that the morphology observed via FIB-SEM is very close to the schematic representation. This demonstrates the effective magnetic alignment of mhBN in silicone. As given in Table 1, the ideal morphology for the ImhBN−silicone is that the platelets should be projected as 1D horizontal rods in the cross-section view and 2D plates in the top view. The cross-section and top-view FIB-SEM images of the ImhBN−silicone are given in parts e and h of Figure 4, respectively. It is shown that, except for some unexpected platelets indicated by red arrows, the observed morphology accords with the ideal morphology. In contrast, in the RmhBN−silicone, the mhBN platelets oriented randomly and both through-plane and in-plane alignment characterizations can be found in the FIB-SEM images. For example, 1D vertical and horizontal rods, which are separately observed in cross sections of TmhBN−silicone and ImhBN−silicone, exist

simultaneously in the cross section of RmhBN−silicone (Figure 4f). Moreover, in the top-view FIB-SEM image (Figure 4i), both 2D plates and 1D rods can be found abundantly.

To further determine the orientation of mhBNs in silicone matrix, XRD analysis was carried out. Figure 5a gives the XRD patterns. It is shown that the peak intensities for the three composites are dramatically different. As reported previously[20] and schematically illustrated in Figure 5b, the horizontally and vertically oriented hBNs are responsible for the (002) and (100) peaks, respectively. Thus, the difference in peak intensities suggests the various degrees of orientation (δ) of mhBNs. δ is estimated by comparing the relative intensity (I) of the (100) peak to the sum of the relative intensities of the (002) and (100) peaks.

$$\delta = \frac{I_{100}}{I_{002} + I_{100}} \times 100\% \tag{1}$$

Table 2 summarizes the values of δ for the three composites. We compare the δ values of RmhBN−silicone and TmhBN−silicone first. It is found that δ of TmhBN−silicone is more than 2 times larger than that of RmhBN−silicone, which suggests the larger amount of through-plane-oriented mhBNs in TmhBN−silicone. Then, δ values of RmhBN−silicone and ImhBN−silicone are compared. The result is that δ of ImhBN−silicone is approximately 5 times lower than that of RmhBN−silicone. The lower value of δ demonstrates that ImhBN−silicone has a larger amount of in-plane-aligned mhBNs and a lower amount of through-plane-aligned mhBNs.
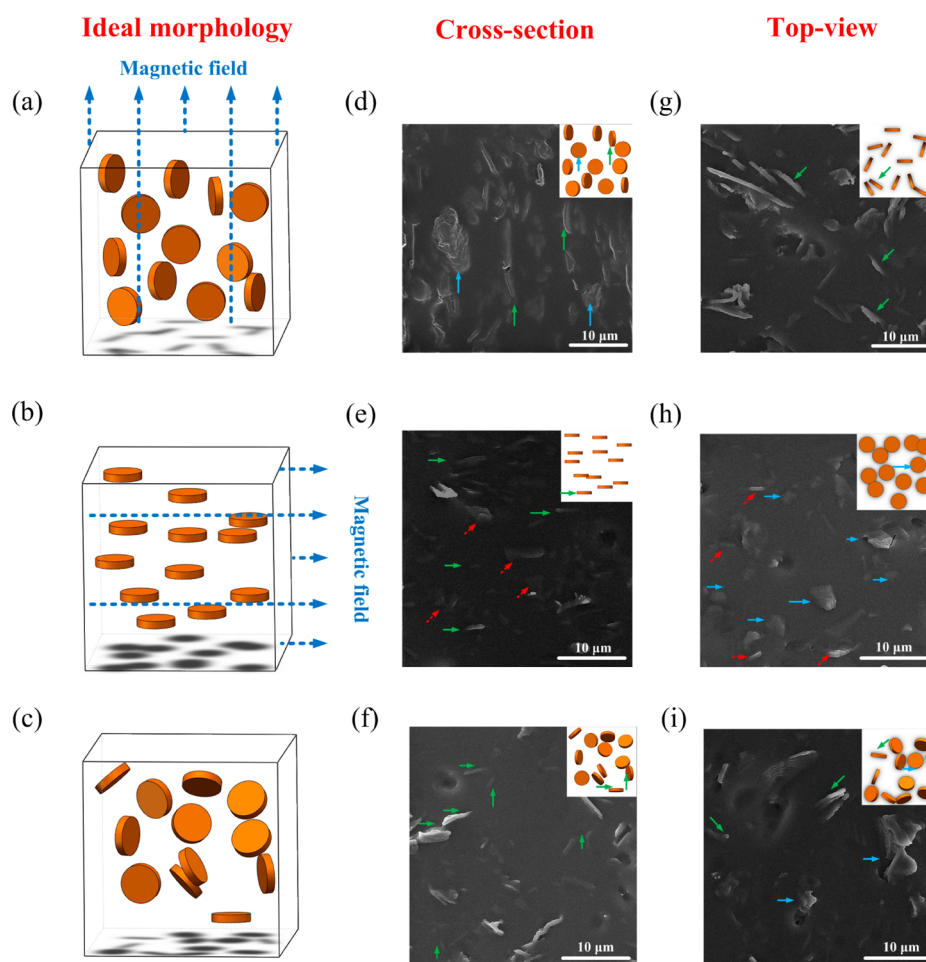
Figure 4. Alignment of mhBN platelets in composites with a volume faction of 9.14%. (a) Schematic and (d) cross-section and (g) top-view FIB-SEM images of composites with through-plane oriented platelets. (b) Schematic and (e) cross-sectional and (h) top-view FIB-SEM images of composites with in-plane oriented platelets. (c) Schematic and (f) and cross-sectional and (i) top-view FIB-SEM images of composites with randomly oriented platelets. 1D rods and 2D plates are indicated by green and blue arrows, respectively, and the unexpected morphology is indicated by red arrows.

Table 1. Representative Morphologies of mhBN Platelets in TmhBN−Silicone, RmhBN−Silicone, and ImhBN−Silicone Composites

	TmhBN−silicone	ImhBN−silicone	RmhBN−silicone
cross section	1D vertical rods and 2D plates	1D horizontal rods	randomly oriented plates or rods
top view	randomly oriented 1D rods	2D plates	randomly oriented plates or rods

Thermal Conductivity of mhBN−Silicone Composites.
We investigate the effect of mhBN orientation on the thermal conductivity of composites. Table 3 gives the measured ρ, C_p, and through-plane thermal diffusivity (α_T) data for the three composites at the volume fraction (f) of 5%, 7.5%, and 9.14%. From the data, k_T can be calculated. Figure 6 shows the measured k_T of TmhBN−silicone, RmhBN−silicone, and ImhBN−silicone. The results demonstrate the same tendency for all composites that k_T increases with the increase of f. This tendency can be explained by the greater contribution of thermal transport through mhBNs at higher f. However, k_T is dramatically different among the three composites with the same f. Figure 6 gives the thermal enhancements of TmhBN−silicone and ImhBN−silicone with reference to RmhBN−silicone, respectively. TmhBN−silicone exhibits 35.4%, 43.6%,

and 44.5% higher k_T for the f at 5%, 7.5% and 9.14%, respectively. The higher k_T of TmhBN−silicone is owing to the formation of efficient thermal pathways made by the mhBN platelets oriented parallel to the heat flux. In sharp contrast, k_T of composites containing the in-plane-aligned mhBNs at those volume fractions are 29.7%, 37.4%, and 37.9% lower compared to the values of RmhBN−silicone. The results illustrate that k_T will be suppressed when the mhBN platelets orient perpendicular to the heat flux.

A theoretical model is applied to analyze the experimental data. The modified effective medium approximation (EMA)[21] is very useful in predicting k_T of composites containing the platelet-shaped fillers. This model takes into account filler geometry and orientation, volume fraction, and thermal boundary resistance (R_b) at the filler−matrix interface. At first, we study the effect of R_b on k_T. It is well-known[5,6,9,21] that R_b arises from the combination of a poor mechanical or chemical adherence at the filler−matrix interface and a thermal expansion mismatch. In this study, the additional iron oxide nanoparticles on the hBN surface are another factor creating R_b at the interface.[10] Figure 7 gives the predicted k_T from EMA with the consideration of R_b, and it can be observed that R_b has an adverse impact on k_T. By fitting the measured k_T to the EMA prediction, the actual R_b of the composites can be extracted
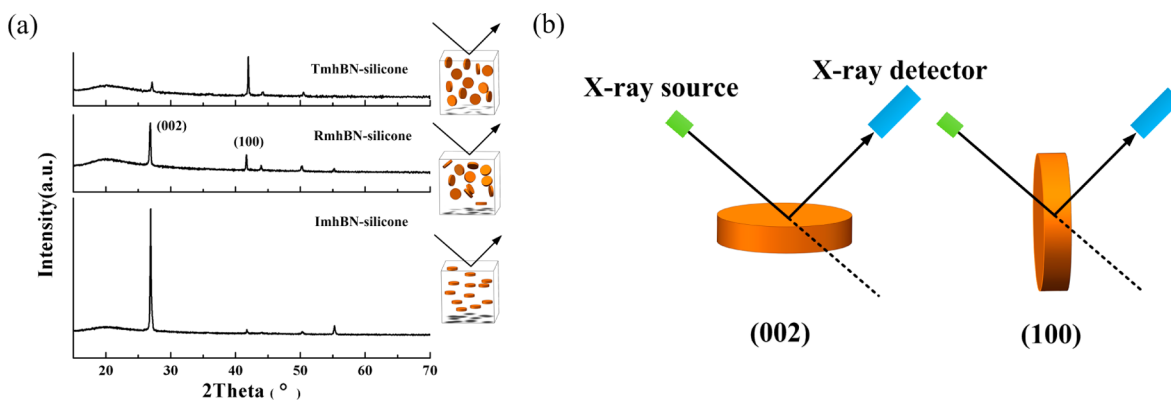
Figure 5. XRD analysis of mhBN−silicone composites. (a) XRD patterns of TmhBN−silicone, RmhBN−silicone, and ImhBN−silicone composites. (b) Illustration of the effect of the orientation of hBN on the XRD pattern.

Table 2. Degree of Orientation of mhBNs of TmhBN−Silicone, RmhBN−Silicone, and ImhBN−Silicone Composites, Respectively

composites	δ (%)
TmhBN−silicone	65.6
RmhBN−silicone	27.2
ImhBN−silicone	5.9

Table 3. Density, Heat Capacity, and Through-Plane Thermal Diffusivity of mhBN−Silicone Composites at Volume Fractions Ranging from 5% to 9.14%

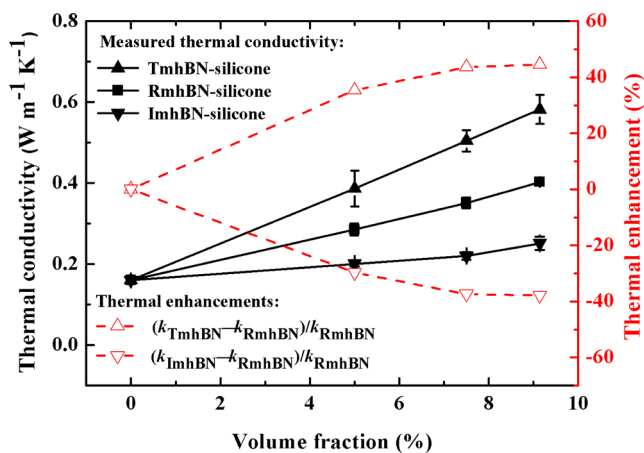| volume fraction (f, %)	density (ρ, g cm^{-3})	heat capacity (C_p, J g^{-1} K^{-1})	through-plane thermal diffusivity$_T$ (α, mm^2 s^{-1})		
			TmhBN	RmhBN	ImhBN
5	1.20	1.36	0.237	0.175	0.123
7.5	1.22	1.33	0.311	0.215	0.135
9.14	1.24	1.31	0.357	0.247	0.154

Figure 6. Thermal conductivities of composites corresponding to thermal enhancements.

(see details in the Supporting Information). Parts a and b of Figure 7 give the fitting results for the TmhBN−silicone and RmhBN−silicone, respectively. R_b for the TmhBN−silicone is found to be 20×10^{-9} m^2 W K^{-1}, which is comparable to the reported value for the polymer composites with through-plane-oriented mhBNs.[10] For the RmhBN−silicone, R_b is fitted to be

300×10^{-9} m^2 W K^{-1}, which is much larger than that of TmhBN−silicone. Such anisotropic R_b has also been observed in hBN−epoxy composites.[10] In addition, it can be found that with the large R_b, thermal transport in RmhBN−silicone composites is suppressed: k_T of the composites at the volume fraction of 5%, 7.5%, and 9.14% are reduced by 10.1%, 11.6%, and 11.4%, respectively.

Figure 8a gives the comparison between the measured and predicted k_T of the composites. For the TmhBN−silicone and RmhBN−silicone, the predictions surely match well with the experiments owing to the fitting. However, it is interesting to note that for the ImhBN−silicone, the predicted k_T is lower than that observed in the experiments. This deviation could be attributed to the inappropriate assumption of the orientation of mhBNs in the ImhBN−silicone composites. The EMA prediction assumes that the platelets are completely in-plane-oriented in the matrix. However, according to the FIB-SEM observations, some mhBN platelets are found to be not aligned to the horizontal direction. These unexpected platelets increase the thermal transport in the composites and hence increase k_T.

We use the theoretical model to further investigate the effect of orientation on k_T. In this model, the orientational characteristic of platelets in the matrix is represented by the parameter $\langle \cos^2 \theta \rangle$, which is given by[21]

$$\langle \cos^2 \theta \rangle = \frac{\int \rho(\theta) \cos^2 \theta \sin \theta \, d\theta}{\int \rho(\theta) \sin \theta \, d\theta} \tag{2}$$

where $\rho(\theta)$ is a distribution function. As schematically shown in Figure 8b, θ is the angle between the material axis X_3 and the local platelet symmetric axis X_3'. As reported previously[21] and schematically illustrated in Figure 8c, $\langle \cos^2 \theta \rangle$ is theoretically equal to 0, $1/3$, and 1 for the composites containing the platelets oriented completely through-plane, randomly, and in-plane. Figure 8a gives the predicted k_T from EMA with the $\langle \cos^2 \theta \rangle$ ranging from 0 to 1. This clearly shows that k_T decreases with the increase of $\langle \cos^2 \theta \rangle$. By fitting the measured k_T to the EMA prediction, the actual $\langle \cos^2 \theta \rangle$ of ImhBN−silicone composites can be extracted (see details in Supporting Information). The fitting result is shown in Figure 8a, and $\langle \cos^2 \theta \rangle$ is found to be $12/15$.

According to the above analysis, the thermal conductivity of the composites is strongly associated with the magnetic alignment of the mhBN platelets. Aligning the platelets parallel to the direction of heat flux can greatly enhance the thermal transport in the composites, due to the formation of conductive
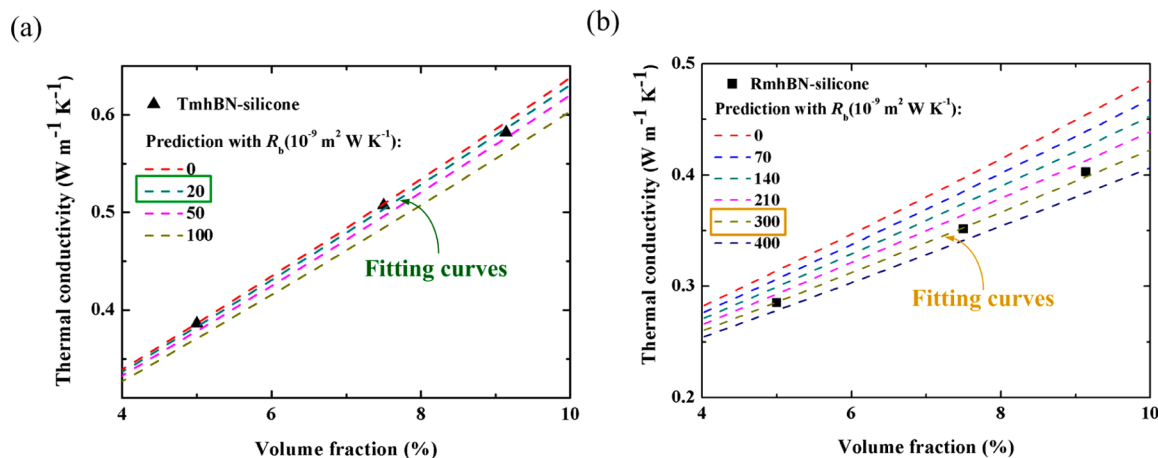
Figure 7. Data fitting to extract the thermal boundary resistance (R_b) of (a) TmhBN−silicone and (b) RmhBN−silicone composites. Black dots, measured through-plane thermal conductivity (k_T) of mhBN−silicone composites; colored dash lines, predicted k_T from effective medium approximation (EMA) with different values of R_b.

4. CONCLUSIONS

This work investigated the thermal conductivity of hBN-filled composites as a function of hBN orientation. At first, hBN platelets were coated with magnetic iron oxide nanoparticles to make them magnetically responsive. Then, various microstructures were achieved within the hBNs-filled composites by applying external magnetic fields. Thermal conductivity was measured for the resulting composites. The modified effective medium approximation was applied to analyze the experimental data. Both experimental and modeling results illustrate that thermal conductivity of the composites is strongly associated with the magnetic alignment of the mhBN platelets. By fitting the measured thermal conductivity to the EMA prediction, the thermal boundary resistance (R_b) at the hBN−silicone interface was extracted. It is found that R_b also changes with hBNs orientation.

■ ASSOCIATED CONTENT

ⓢ Supporting Information

Theoretical model for the prediction of the thermal conductivity of composites and the extraction of thermal boundary resistance (R_b) and $\langle \cos^2 \theta \rangle$. The Supporting Information is available free of charge on the ACS Publications website at DOI: 10.1021/acsami.5b03007.

■ AUTHOR INFORMATION

Corresponding Author
*E-mail: luoxb@hust.edu.cn.

Author Contributions

The manuscript was written through contributions of all authors. All authors have given approval to the final version of the manuscript.

Notes

The authors declare no competing financial interest.
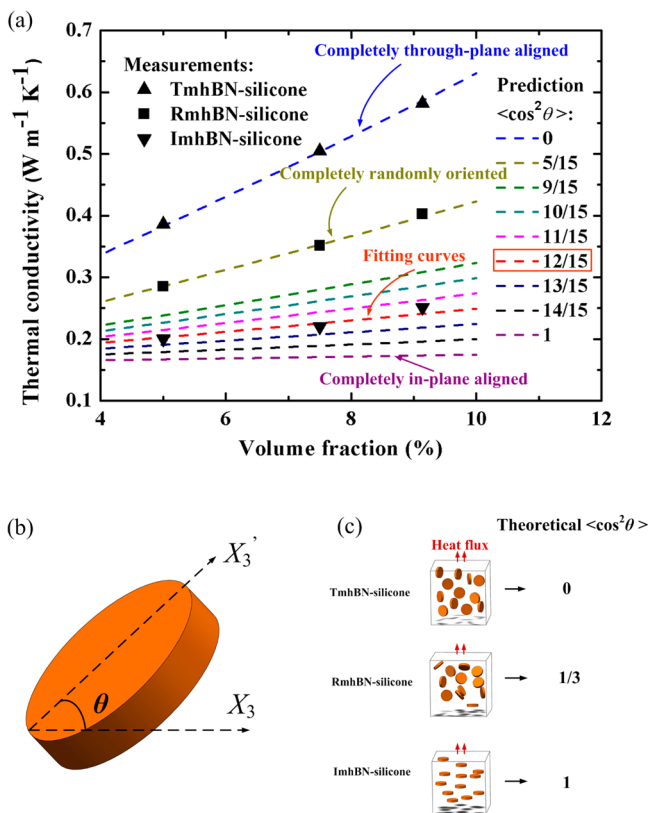
■ ACKNOWLEDGMENTS

Figure 8. (a) Comparison between the measured and predicted through-plane thermal conductivity (k_T) of the composites and data fitting to extract $\langle \cos^2 \theta \rangle$ of ImhBN−silicone composites. Black dots, measured k_T of TmhBN−silicone, RmhBN−silicone, and ImhBN−silicone composites; colored dash lines, predicted k_T from EMA with the $\langle \cos^2 \theta \rangle$ ranging from 0 to 1. (b) Schematic of a platelet with the angle θ. (c) Theoretical values of $\langle \cos^2 \theta \rangle$ for the composites containing completely through-plane-oriented, in-plane-oriented, and randomly oriented platelets, respectively.

networks and the reduced R_b. In contrast, when the orientation of platelets is perpendicular to the heat flux direction, thermal transport will be highly suppressed.

ments, and Mr. Leng Zongyuan from Ferrotec for providing iron oxide nanoparticles.

■ REFERENCES

(1) Lu, D.; Wong, C. P. *Materials for Advanced Packaging*; Springer: New York, 2009.

(2) Wong, C. P.; Moon, K. S.; Li, Y. *Nano-Bio-Electronic, Photonic and MEMS Packaging*; Springer: New York, 2010.

(3) Liu, S.; Luo, X. B. *LED Packaging for Lighting Applications: Design, Manufacturing, and Testing*; John Wiley & Sons Press: New York, 2011.

(4) Moore, A. L.; Shi, L. Emerging Challenges and Materials for Thermal Management of Electronics. *Mater. Today* **2014**, *17*, 163−174.

(5) Prasher, R. S.; Shipley, J.; Prstic, S.; Koning, P.; Wang, J. L. Thermal Resistance of Particle Laden Polymeric Thermal Interface Materials. *J. Heat Transfer* **2003**, *125*, 1170−1177.

(6) Prasher, R. S. Thermal Interface Materials: Historical Perspective, Status, and Future Directions. *Proc. IEEE* **2006**, *94*, 1571−1586.

(7) Otiaba, K. C.; Ekere, N. N.; Bhatti, R. S.; Mallik, S.; Alam, M. O.; Amalu, E. H. Thermal Interface Materials for Automotive Electronic Control Unit: Trends, Technology and R&D Challenges. *Microelectron. Reliab.* **2011**, *51*, 2031−2043.

(8) Mallik, S.; Ekere, N.; Best, C.; Bhatti, R. Investigation of Thermal Management Materials for Automotive Electronic Control Units. *Appl. Therm. Eng.* **2011**, *31*, 355−362.

(9) Yuan, C.; Luo, X. B. A Unit Cell Approach To Compute Thermal Conductivity of Uncured Silicone/Phosphor Composites. *Int. J. Heat Mass Transfer* **2013**, *56*, 206−211.

(10) Lin, Z. Y.; Liu, Y.; Raghavan, S.; Moon, K. S.; Sitaraman, S. K.; Wong, C. P. Magnetic Alignment of Hexagonal Boron Nitride Platelets in Polymer Matrix: Toward High Performance Anisotropic Polymer Composites for Electronic Encapsulation. *ACS Appl. Mater. Interfaces* **2013**, *5*, 7633−7640.

(11) Takahashi, F.; Ito, K.; Morikawa, J.; Hashimoto, T.; Hatta, I. Characterization of Heat Conduction in a Polymer Film. *Jpn. J. Appl. Phys.* **2004**, *43*, 7200−7204.

(12) Li, T. L.; Hsu, S. L. C. Enhanced Thermal Conductivity of Polyimide Films via a Hybrid of Micro- and Nano-Sized Boron Nitride. *J. Phys. Chem. B* **2010**, *114*, 6825−6829.

(13) Li, T. L.; Hsu, S. L. C. Preparation and Properties of Thermally Conductive Photosensitive Polyimide/Boron Nitride Nanocomposites. *J. Appl. Polym. Sci.* **2011**, *121*, 916−922.

(14) Sato, K.; Horibe, H.; Shirai, T.; Hotta, Y.; Nakano, H.; Nagai, H.; Mitsuishi, K.; Watari, K. Thermally Conductive Composite Films of Hexagonal Boron Nitride and Polyimide with Affinity-Enhanced Interfaces. *J. Mater. Chem.* **2010**, *20*, 2749−2752.

(15) Lin, T. H.; Huang, W. H.; Jun, I. K.; Jiang, P. Bioinspired Assembly of Surface-Roughened Nanoplatelets. *J. Colloid Interface Sci.* **2010**, *344*, 272−278.

(16) Libanori, R.; Munch, F. H. L.; Montenegro, D. M.; Studart, A. R. Hierarchical Reinforcement of Polyurethane-Based Composites with Inorganic Micro- and Nanoplatelets. *Compos. Sci. Technol.* **2012**, *72*, 435−445.

(17) Munch, E.; Launey, M. E.; Alsem, D. H.; Saiz, E.; Tomsia, A. P.; Ritchie, R. O. Tough, Bio-Inspired Hybrid Materials. *Science* **2008**, *322*, 1516−1520.

(18) Erb, R. M.; Libanori, R.; Rothfuchs, N.; Studart, A. R. Composites Reinforced in Three Dimensions by Using Low Magnetic Fields. *Science* **2012**, *335*, 199−204.

(19) Erb, R. M.; Son, H. S.; Samanta, B.; Rotello, V. M.; Yellen, B. B. Magnetic Assembly of Colloidal Superstructures with Multipole Symmetry. *Nature* **2009**, *457*, 999−1002.

(20) Zhi, C. Y.; Bando, Y.; Tan, C. C.; Golberg, D. Effective Precursor for High Yield Synthesis of Pure BN Nanotubes. *Solid State Commun.* **2005**, *135*, 67−70.

(21) Nan, C. W.; Birringer, R.; Clarke, D. R.; Gleiter, H. Effective Thermal Conductivity of Particulate Composites with Interfacial Thermal Resistance. *J. Appl. Phys.* **1997**, *81*, 6692−6699.